expected (*28*). However, the ratio of heat to freshwater buoyancy fluxes is variable in large-scale maps (*28*) and in time series at a point (*29*), so internal ocean dynamics may be required to establish a uniform large-scale density ratio. Observational confirmation of our hypothesis of the existence of a staircase-like temperature-salinity relationship would require tows long enough to cross a number of strong density fronts and in different ocean basins.

References and Notes

1. C. O. D. Iselin, *Trans. Am. Geophys. Union* **20**, 414 (1939).
2. The mixed layer is a layer at the ocean's surface that is relatively vertically uniform in properties such as temperature and salinity. The turbulence that mixes this layer is a result of wind and surface cooling.
3. The thermocline is a region of relatively high stratification below the mixed layer.
4. H. Stommel, *Proc. Natl. Acad. Sci. U.S.A.* **76**, 3051 (1979).
5. J. R. Luyten, J. Pedlosky, H. Stommel, *J. Phys. Oceanogr.* **13**, 292 (1983).
6. M. C. Gregg, *J. Geophys. Res.* **94**, 9686 (1989).
7. J. R. Ledwell, A. J. Watson, C. S. Law, *Nature* **364**, 701 (1993).
8. G. I. Roden, *J. Phys. Oceanogr.* **5**, 557 (1975).
9. ———, *Ann. Geophys.* **2**, 399 (1984).
10. H. M. Stommel, *J. Phys. Oceanogr.* **23**, 142 (1993).
11. ——— and W. R. Young, *ibid.*, p. 151.
12. W. R. Young, *ibid.* **24**, 1812 (1994).
13. L. Chen and W. R. Young, *ibid.* **25**, 3064 (1995).
14. R. Ferrari and W. R. Young, *J. Mar. Res.* **55**, 1069 (1997).
15. The Earth's rotation should act to limit the slumping at horizontal scales larger than the Rossby radius of deformation (the scale above which the effects of rotation become important). Although slumping should occur at large scales, it need not proceed until isopycnals are horizontal.
16. R. M. Samelson and C. A. Paulson, *J. Geophys. Res.* **93**, 2237 (1988).
17. R. Pollard, *Nature* **323**, 433 (1986).
18. Sensors for measuring temperature and conductivity (which is used to calculate salinity) must be calibrated to account for differences in time constants of the sensors. We used the methods of Lueck and Picklo [R. G. Lueck and J. J. Picklo, *J. Atmos. Oceanic Technol.* **7**, 756 (1990)] and Rudnick and Luyten [D. L. Rudnick and J. R. Luyten, *J. Geophys. Res.* **101**, 923 (1996)].
19. Temperature-salinity variability below the mixed layer is caused by internal waves, stirring, and mixing. The isobar and isopycnal tows are intended to study these processes.
20. I. Daubechies, *Ten Lectures on Wavelets*, CBMS-NSF Regional Conference Series in Applied Mathematics (Society for Industrial and Applied Mathematics, Philadelphia, 1992); M. Farge, *Annu. Rev. Fluid Mech.* **24**, 395 (1992). The wavelet transform may be thought of as convolutions with a set of functions (wavelets) of changing frequency content. An important feature of a wavelet is that its quality factor Q, defined as the ratio of the wavelet's central wave number to its spread in wave number, is constant. Wavelets are derived by dilation of the so-called mother wavelet. Here we choose the Morlet wavelet (a plane wave modulated by a Gaussian envelope) with $Q = 2\sqrt{2}\pi$.
21. I. Langmuir, *Science* **87**, 119 (1938).
22. R. A. Weller *et al.*, *ibid.* **227**, 1552 (1985).
23. K. E. Brainerd and M. C. Gregg, *J. Geophys. Res.* **98**, 22645 (1993).
24. R. W. Schmitt, *Annu. Rev. Fluid Mech.* **26**, 255 (1994).
25. ———, *J. Phys. Oceanogr.* **11**, 1015 (1981).
26. L. G. Chen, *ibid.* **25**, 691 (1995). In winter between the 7° and 17°C isotherms, estimates of *R* are 1.9 averaged over the North Pacific and 1.4 at the longitude of our measurements (140°W).
27. Compensated temperature and salinity features are often found near strong density fronts [D. L. Rudnick and J. R. Luyten, *J. Geophys. Res.* **101**, 923 (1996)].
28. R. W. Schmitt, P. S. Bogden, C. E. Dorman, *J. Phys. Oceanogr.* **19**, 1208 (1989).
29. S. P. Anderson, R. A. Weller, R. B. Lukas, *J. Clim.* **9**, 3056 (1996).

30. We thank Lloyd Regier, Lyn Harris, and John Paoli for their efforts in support of the observational program. Thanks are due to Bill Young for inspiring discussions. We gratefully acknowledge the support of the National Science Foundation under grant OCE95-29752.

7 October 1998; accepted 4 December 1998

Transient Phase–Induced Nucleation

E. B. Sirota* and A. B. Herhold

A transient metastable rotator phase occurring on crystallization of hexadecane into its triclinic phase from the supercooled melt was directly observed with time-resolved synchrotron x-ray scattering. In this system, the limit of supercooling (the crystallization temperature) is determined by the thermodynamic stability of the transient phase with respect to the liquid. The crystallization kinetics of the homologous series of n-alkanes was measured and explained in terms of a crossover from stability to "long-lived" metastability to transient metastability. This crossover allowed further confirmation of the nature of the transient phase.

Materials often crystallize into metastable forms when cooling from the melt. Once formed, a metastable phase may remain stable indefinitely even for very large undercoolings. However, nucleation could occur to create a transient phase that converts to the stable form during some stage of growth. In such a case, there may be no temperature at which the metastable phase will remain indefinitely. Transient phases are intrinsically difficult to observe and their study has been limited (*1–3*). Such transient states are not only intermediate forms on the path to the final state (*4*) but they can be key to understanding the crystallization behavior. In particular, the nucleation temperature of the transient state can determine the observed crystallization or precipitation temperature of the stable phase, that is, the limit of supercooling. In addition, the properties of the metastable phase can determine the growth morphology of the crystal; for example, enhanced chain mobility in the metastable hexagonal phase (which is stable at high pressure) may cause lamellar thickening in polyethylene (*3*).

The n-alkanes (C_nH_{2n+2}, abbreviated C_n) are not only interesting in their own right because of their varied behavior but are the principal component of petroleum waxes and the building block of many derivative molecules whose properties are strongly influenced by their alkyl component (*5, 6*). The n-alkanes exhibit an even-odd effect in their melting points and crystal structures (*5, 7, 8*), but the kinetics and observed hysterisis have remained unexplained. Here we show that the stability of the transient phase can be optimized for an appropriate choice of alkane chain length. We provide an example of transient phase–induced nucleation and explain the kinetic behavior of n-alkane crystallization in terms of a crossover from "long-lived" to transient metastability.

In general, alkanes exhibit rotator phases below the melting temperature (*6, 9, 10*). For *n*-even alkanes, in the equilibrium phase diagram the rotator (R) phases are replaced at lower *n* by a triclinic (T) nonrotator crystal phase. Bulk melts of the *n*-odd alkanes ($15 \leq n \leq 29$) exhibit a liquid-rotator (L→R) transition with negligible supercooling (*7, 8, 10*). The lack of supercooling in the melts has been suggested (*8, 11*) to be related to the presence of a surface monolayer R phase that occurs in equilibrium at the liquid-vapor interface a few Celsius degrees above the crystallization temperature (*12*), and this surface R phase would serve as an ideal nucleation site for the bulk R phase (*13*). The equilibrium melting points exhibit a significant even-odd effect that can be associated with whether melting occurs from the T crystal (*n*-even) or from the R phase (*n*-odd) (*7, 8*). However, the even-odd effect disappears when observed freezing temperatures are considered (Fig. 1) because the *n*-even alkanes with high melting points supercool, whereas the *n*-odd alkanes, which crystallize into the R phase, do not. Is it a coincidence that the amount of supercooling for *n*-even alkanes is equal and opposite to the even-odd difference in the melting temperatures? It had been hypothesized that it is not (*8*). We now demonstrate this correspondence experimentally and show that short *n*-even alkanes crystallize through a transient R phase.

Exxon Research and Engineering Company, Corporate Research Science Laboratory, Route 22 East, Annandale, NJ 08801, USA.

*To whom correspondence should be addressed. E-mail: ebsirot@erenj.com

We studied the time-dependent x-ray scattering (*14*) of C_{16}, which exhibits unambiguous supercooling from the melt and is energetically far away from exhibiting a stable bulk R phase. In contrast, C_{22} shows a stable R phase on heating and cooling; C_{20}, only on cooling; and C_{18} not at all. The stable form of C_{16} is the T crystal phase in which the molecules are tilted with respect to the layers by 19.4° (*15*). The 001 reflection at $q = 2\pi/d = 0.305$ Å^{-1} corresponds to a layer spacing of $d = 20.6$ Å. The in-plane packing of this phase gives rise to principal reflections at $q = 1.374$ Å^{-1}, 1.658 Å^{-1}, and 1.753 Å^{-1} as well as mixed reflections. The position-sensitive detector (PSD) was usually centered at $q = 0.29$ Å^{-1} (scattering angle, $2\theta = 4°$) to detect the 001 lamellar reflection, and a few times at $q = 1.58$ Å^{-1} ($2\theta = 22°$) to probe the higher q in-plane reflections.

Because nucleation is a stochastic event and any single crystallite would only be observed if it were oriented at a correct angle with respect to the detector, we automated the cooling process and recorded 85 cycles. The sample was heated ~10°C above the melting temperature T_m and then cooled just below the point at which crystallization could be observed. With a slow cooling rate of ~0.03°C/min, the onset of the T phase was observed at 16.51°C. We recorded data from the PSD averaged over 10-s intervals, cooling at 0.5°C/min, to a final T of 16.4°C. The first peaks appeared at the same time (±15 s) within each cycle.

We observed scattering peaks from a transient phase for 9 out of the 85 cooling cycles. The scattering at low angles as a function of time for one such case is shown in Fig. 2. A peak develops at $q = 0.286$ Å^{-1} and subsequently disappears as the peak at $q = 0.305$ Å^{-1} develops. The transient peak is visible for ~20 s, and its position suggests untilted molecules, that is, $\cos^{-1}(0.286/0.305) = 20.3°$. Three other cooling cycles gave similar results in which the peak intensity of the transient phase at $q = 0.286$ Å^{-1} was weaker but still unambiguous (comparable to the fourth curve in Fig. 2) and with lifetimes of ≤10 s. Four cycles gave very weak peaks at $q = 0.286$ Å^{-1} for ≤10 s. Once, the transient phase remained for almost 8 min, and in Fig. 3 we show high-angle scans taken during that cooling run. The three scans shown were taken at 30-s intervals. Before these scans, the lamellar peak was at $q = 0.286$ Å^{-1}, and after these scans, at $q = 0.305$ Å^{-1}. The pattern shown in Fig. 3C is that expected for the stable T phase of C_{16}. The peak positions of the transient phase appeared at $q = 1.498$ Å^{-1} and $q = 1.632$ Å^{-1}. Coexistence of both the phases and the peak positions of the transient phase are distinct from any peaks exhibited by the stable T crystal phase (Fig. 3B).

The n-odd alkanes ($n \leq 21$) exhibit the orthorhombic R_I rotator phase with molecules untilted with respect to the layers (*9*). To identify the observed transient phase, we plotted (Fig. 3, inset) the peak positions of the R_I phase just below the freezing temperature T_f for n-odd alkanes, along with the positions observed here for C_{16}. The peak positions observed for the transient phase correspond to the interpolated peak position expected for the R phase. Also shown are the peak positions of the untilted, orthorhombic, herringbone crystal phase (nonrotator) of the n-odd alkanes, which unambiguously differ from those of the transient phase.

A transient R phase occurs upon crystallization from the supercooled melt. The distribution in lifetimes from these observations leaves us with another set of questions: If the R phase nucleates first, how long will that phase last and what determines when conversion occurs to the stable T phase? Insight is provided by systematic x-ray scattering measurements of the chain-length dependence of the various transitions (Fig. 1) (*16*). Temperature scanning rates as slow as 0.007°C/min were used to obtain systematic transition temperatures. Crystallization is first encountered at T_f (cooling slowly at 0.03°C/min). For the chain lengths where the L→R transition can be observed in both directions (that is, even-$n \geq 20$ and odd-n), $T_{R \rightarrow L}$ and T_f agree to within ~0.1°C, consistent with the lack of supercooling observed for this transition (*7, 8, 10*). The points labeled $T_{T \rightarrow L}$ show where the T phase melts to the liquid (even-$n \leq 20$). $T_{T \rightarrow R}$ is where the T phase transforms to the R phase on heating (even-$n \geq 22$). $T_{R \rightarrow T}$ is the average temperature at which a rotator R transforms to the T when cooling at ~0.07°C/min (*17*).

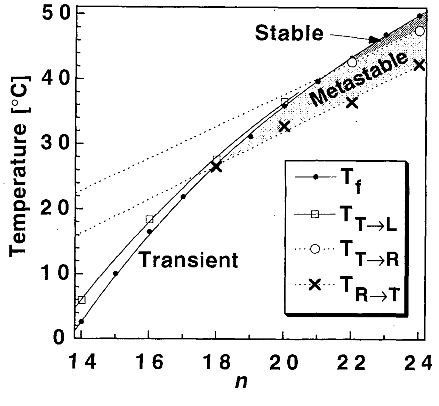

Fig. 1. Phase diagram of the n-alkanes. The closed circles are the freezing temperatures T_f. The open squares are the melting temperature ($T_{T \rightarrow L}$) for those n-alkanes that melt from the triclinic phase. The melting temperatures for the other n-alkanes coincide with their freezing temperatures. The open circles are the T-R phase transformation temperatures on heating ($T_{T \rightarrow R}$), and the crosses are the average R-T transition temperatures ($T_{R \rightarrow T}$) on cooling at 0.05°C/min. The dashed lines are lines $T_{R \rightarrow T} = 37.71 + 2.47(n - 20)$ and $T_{T \rightarrow R} = 31.96 + 2.60(n - 20)$, and the solid curves are fits to the empirical form (*23*) yielding $T_f = 131.0(n - 13.66)/(n + 3.15)$ and $T_{T \rightarrow L} = 134.7(n - 13.13)/(n + 5.39)$. The regions labeled "Stable," "Metastable," and "Transient" refer to the stability of the R phase for n-even alkanes.

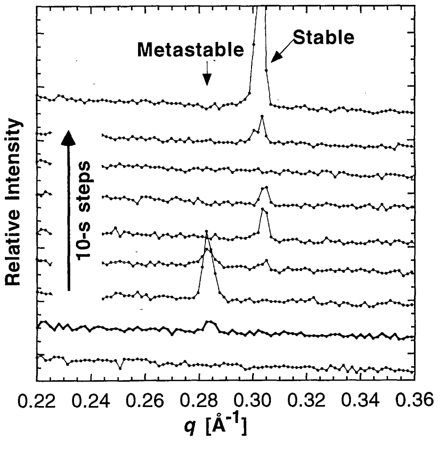

Fig. 2. Scattering intensity versus q as a function of time for one cooling run, showing the 001 lamellar peak of C_{16} during crystallization. The metastable peak develops at $q = 0.286$ Å^{-1}, and the stable peak later appears at $q = 0.305$ Å^{-1}. The scans were taken in 10-s steps and are offset vertically. In the early stages of crystallization only a few crystallites are present. These may rotate and must be oriented fortuitously to be detected; therefore, the total peak intensity does not quantitatively represent the total crystallized fraction, and the nonmonotonic increase in peak intensity in this sequence is not of significance here.

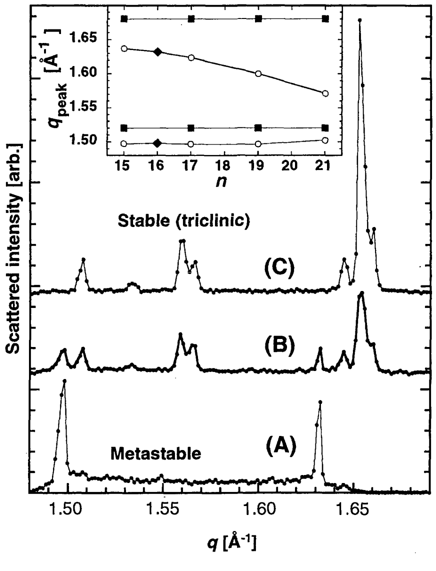

Fig. 3. (**A** to **C**) Scattering intensity versus q at 30-s intervals showing the in-plane peaks of C_{16} transforming from the transient metastable phase to the stable phase (arb., arbitrary units) (**Inset**) The peak positions in the stable R_I phase just below the melting temperature (circles) and in the low-temperature herringbone crystal phase (squares) as a function of n. The observed positions of the peaks in the transient phase of C_{16} (diamonds) are consistent with the R phase.

We can associate $T_{T \rightarrow R}$ with the equilibrium temperature of the T↔R transition because this transition does not superheat, as confirmed by thermal measurements with adiabatic scanning calorimetry (*10*). $T_{R \rightarrow T}$ is the temperature below which the R→T transition is likely to occur on a "reasonable" time scale. $T_{R \rightarrow T}$ and $T_{T \rightarrow R}$ are essentially parallel (Fig. 1), showing that the R→T transition supercools in bulk by ~6°C.

If nucleation to the R phase occurs at T_f, then for C_{16} this is well below the $T_{R \rightarrow T}$ line and the R→T transformation will proceed rapidly. For C_{18}, $T_{R \rightarrow T}$ is only slightly greater than T_f, meaning that it will certainly occur on laboratory time scales, but it can be expected to occur more slowly. Indeed, our x-ray scattering measurements revealed a transient R phase in C_{18}, which was stable for an average of ~3 min with a wide distribution whose tail extended beyond 30 min (*16*).

It is thus apparent that the chain length–dependent phase diagram contains a crossover in the *n*-even alkanes from a stable R phase ($n \geq 24$) to a metastable R phase ($n = 20, 22$) to a transient R phase ($n \leq 18$). For C_{18} the R phase is just on the border of transience and is rather long lived. For C_{16} it is observable with time-dependent synchrotron scattering. For C_{14} where T_f is 20°C below $T_{T \rightarrow R}$, one would not expect to directly observe the transient phase; however, it nevertheless controls T_f. In Fig. 4, we show schematically the relative free energies of the three phases for the three scenarios and illustrate the path taken on cooling and heating.

We have shown that the temperature at which the supercooled liquid transforms to the T phase lying on the same curve as where the R phase would be stable with respect to the liquid is no coincidence, but rather, the crystallization of the T phase is mediated by a transient R phase. The recognition of the importance of such transient-phase nucleation may help explain not only crystallization from the melt, but also crystallization from solutions and homogeneous nucleation from the melt. If we were to suppose that homogeneous nucleation were limited by the energy barrier to nucleating in a transient R phase and relate the observed crystallization temperature to $T_{R \rightarrow L}$ rather than to $T_{T \rightarrow L}$, the even-odd variation observed in the undercooling (*18*) smoothes out. This observation suggests that the low interfacial energies of the R phases may play a major role in crystal nucleation, not only with respect to the T crystal phase of the *n*-even series, but also with respect to the orthorhombic crystal phases of the *n*-odd alkanes, mixtures, and solutions. Growth morphologies also depend on the crystal structure (*19*); thus, growth in a transient phase may affect morphology. It has been suggested that the solid-liquid interfaces of the low-temperature crystal phase may be a rotator-like state (*20*). Thus, the transient phase may also manifest itself at growth fronts.

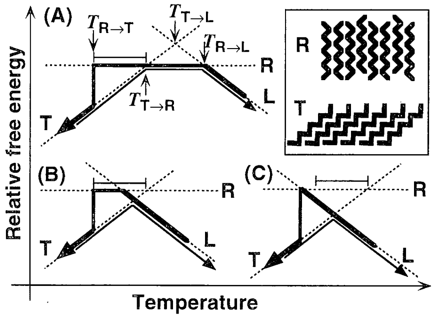

Fig. 4. Schematic showing the relative free energy versus temperature for **(A)** a stable R phase (C_{24}), **(B)** a metastable R phase (C_{20}), and **(C)** a transient R phase (C_{16}). The dashed lines represent the equilibrium free energy curves for the three phases. The heavy and light solid lines represent the paths taken on cooling and heating, respectively. The bracket represents the difference between $T_{T \rightarrow R}$ and $T_{R \rightarrow T}$. **(Inset)** Schematic representing the structure of the two ordered phases.

In addition to mediating crystallization on slow cooling, such transient phases may be locked in by deep quenching. Indeed, in the cycloparaffin nonadecylcyclohexane, an R phase that is transient on slow cooling remains indefinitely on deep quenching (*21*). This result suggests that some phases that are reported to be formed only by deep quenching may be transient states mediating crystallization at higher temperatures.

Some recent studies of nucleation suggest the occurrence of precursor phases that have a density higher than that of the liquid, but where the symmetry of the ordered phase is not fully developed (*2, 22*). The R phases are similar in that their density is higher than the liquid and the symmetry is higher than that of the stable crystal (both quantities being intermediate).

Within the context of classical nucleation theory (*18*), nucleation will occur in a metastable phase if $\sigma_{ml}^3/[\Delta S_{ml}(T - T_{ml})]^2 < \sigma_{sl}^3/[\Delta S_{sl}(T - T_{sl})]^2$ at the crystallization temperature, where σ are the surface energies, ΔS are the transition entropies, and s, m, and l refer to stable, metastable, and liquid. Even without the heterogeneous mechanism (*13*), which in this case reduces the effective surface energy barrier, $\sigma_{ml} < \sigma_{sl}$ is a likely condition, especially for phases of intermediate order. Thus, transient phase–induced nucleation may indeed be a widespread effect.

References and Notes

1. M. Sutton *et al.*, *Phys. Rev. Lett.* **62**, 288 (1989).
2. P. R. ten Wolde, M. J. Ruiz-Montero, D. Frenkel, *ibid.* **75**, 2714 (1995); Y. C. Shen and D. W. Oxtoby, *ibid.* **77**, 3585 (1996).
3. M. Hikosaka *et al.*, *J. Macromol. Sci.* **B31**, 87 (1992); S. Rastogi *et al.*, *Macromolecules* **24**, 6384 (1991); A. Keller, M. Hikosaka, S. Rastogi, *Phys. Scr.* **T66**, 243 (1996); A. Keller *et al.*, *J. Mater. Sci.* **29**, 2579 (1994); A. Keller and S. Z. D. Cheng, *Polymer* **39**, 4461 (1998).
4. W. Ostwald, *Z. Physik. Chem.* **22**, 286 (1897).
5. D. M. Small, *The Physical Chemistry of Lipids* (Plenum, New York, 1986).
6. G. Ungar, *Macromolecules* **19**, 1317 (1986); E. B. Sirota, *Langmuir* **13**, 3849 (1997).
7. A. M. Taggart, F. Voogt, G. Clydesdale, K. J. Roberts, *Langmuir* **12**, 5722 (1996).
8. E. B. Sirota, *ibid.* **14**, 3133 (1998).
9. B. Ewen, G. R. Strobl, D. Richter, *Faraday Discuss. Chem. Soc.* **69**, 19 (1980); J. Doucet, I. Denicolo, A. Craievich, *J. Chem. Phys.* **75**, 1523 (1981); I. Denicolo, J. Doucet, A. F. Craievich, *ibid.* **78**, 1465 (1983); G. Ungar, *J. Phys. Chem.* **87**, 689 (1983); E. B. Sirota, H. E. King Jr., D. M. Singer, H. H. Shao, *J. Chem. Phys.* **98**, 5809 (1993); E. B. Sirota, H. E. King Jr., H. H. Shao, D. M. Singer, *J. Phys. Chem.* **99**, 798 (1995); E. B. Sirota and H. E. King Jr., *Science* **281**, 143 (1998), full text at www.sciencemag.org/cgi/content/full/281/5374/143a. The R phases are lamellar crystals that lack long-range order in the rotational degree of freedom of the molecules about their long axes.
10. E. B. Sirota and D. M. Singer, *J. Chem. Phys.* **101**, 10873 (1994).
11. A. Weinstein and S. A. Safran, *Phys. Rev. E* **53**, R45 (1996).
12. J. C. Earnshaw and C. J. Hughes, *Phys. Rev. A* **46**, 4494 (1992); X. Z. Wu *et al.*, *Science* **261**, 1018 (1993); B. M. Ocko *et al.*, *Phys. Rev. E* **55**, 3164 (1997); H. Gang *et al.*, *Europhys. Lett.* **43**, 314 (1998).
13. In this report, we do not concentrate on the mechanism that causes the R phase not to supercool but simply assume that some inherent heterogeneous mechanism is at work. Ubiquitous tiny bubbles in most bulk situations could serve as such heterogeneous sites.
14. Experiments were performed at the National Synchrotron Light Source on Exxon's beamline X10A with 8-keV radiation and a Braun position-sensitive one-dimensional detector (PSD). The PSD was located 70 cm from the sample and had an active length of 5 cm and width of 1 cm. A small quantity (~0.8 mg) of C_{16} (Aldrich, >99% anhydrous) was placed at the bottom of a quartz capillary that was contained in a temperature-controlled copper cell. The sample was small enough to be entirely illuminated by the 1.5-mm (horizontal) by 1-mm (vertical) beam defined by slits.
15. S. C. Nyburg, F. M. Pickard, N. Norman, *Acta Crystallogr.* **B32**, 2289 (1976).
16. These x-ray scattering measurements were performed with a rotating anode x-ray generator. The samples were contained in a 2-mm-thick copper sample holder with Be windows in a temperature-controlled oven. All materials were >99% pure from Aldrich. Temperature gradients in the oven lead to absolute uncertainties of <0.1°C. The details of how each temperature was obtained will be reported elsewhere (E. B. Sirota and A. B. Herhold, in preparation).
17. $T_{R \rightarrow T}$ is the one transition temperature depicted here that has some cooling-rate dependence (beyond instrumental broadening). It is also stochastic in that the temperature at which it occurs during any one run may vary by ~1°C.
18. Homogeneous nucleation measurements made with the emulsion technique to isolate nuclei result in supercooling of 12 to 15°C [D. Turnbull and R. L. Cormia, *J. Chem. Phys.* **34**, 820 (1961); M. J. Oliver and P. D. Calvert, *J. Cryst. Growth* **30**, 343 (1975); D. R. Uhlmann, G. Kritchevsky, R. Straff, G. Scherer, *J. Chem. Phys.* **62**, 4896 (1975)].
19. P. Bennema *et al.*, *J. Cryst. Growth* **121**, 679 (1992); X. Y. Liu and P. Bennema, *J. Appl. Cryst.* **26**, 229 (1993); *J. Cryst. Growth* **135**, 209 (1994).
20. X. Y. Liu and P. Benemma, *J. Chem. Phys.* **97**, 3600 (1992); T. Yamamoto, *J. Chem. Soc. Faraday Trans.* **91**, 2559 (1995).
21. A. B. Herhold, E. B. Sirota, M. Varma-Nair, in preparation.
22. K. Schatzel and B. Ackerson, *Phys. Rev. Lett.* **68**, 337 (1992); M. Imai, K. Kaji, T. Kanaya, Y. Sakai, *Phys. Rev. B* **52**, 12696 (1995); T. A. Ezquerra, E. Lopez-Cabarcos, B. S. Hsiao, F. J. Balta-Calleja, *Phys. Rev. E* **54**, 989 (1996); N. J. Terrill *et al.*, *Polym. Commun.* **39**, 2381 (1998); P. D. Olmsted *et al.*, *Phys. Rev. Lett.* **81**, 373 (1998).

23. M. G. Broadhurst, *J. Chem. Phys.* **36**, 2578 (1962).
24. We acknowledge discussions with H. E. King Jr., M. Deutsch, S. Srinivas, and J. Hutter and the technical assistance of S. Bennett and W. A. Gordon. The National Synchrotron Light Source at Brookhaven National Laboratory is supported by the U.S. Department of Energy, Division of Mathematical and Chemical Sciences.

21 September 1998; accepted 11 December 1998

Recruitment of a *hedgehog* Regulatory Circuit in Butterfly Eyespot Evolution

David N. Keys,* David L. Lewis,* Jane E. Selegue, Bret J. Pearson, Lisa V. Goodrich, Ronald L. Johnson,† Julie Gates,‡ Matthew P. Scott, Sean B. Carroll§

The origin of new morphological characters is a long-standing problem in evolutionary biology. Novelties arise through changes in development, but the nature of these changes is largely unknown. In butterflies, eyespots have evolved as new pattern elements that develop from special organizers called foci. Formation of these foci is associated with novel expression patterns of the Hedgehog signaling protein, its receptor Patched, the transcription factor Cubitus interruptus, and the *engrailed* target gene that break the conserved compartmental restrictions on this regulatory circuit in insect wings. Redeployment of preexisting regulatory circuits may be a general mechanism underlying the evolution of novelties.

To understand the origin of evolutionary novelties, the developmental and genetic mechanisms that produce new structures and patterns must be elucidated (*1*). One fundamental issue to be addressed is the extent to which novelty arises from either the redeployment of preexisting developmental programs or the separate recruitment of selected individual genes into new programs. The eyespots on butterfly wings are a recently derived evolutionary novelty that arose in a subset of the Lepidoptera and play an important role in predator avoidance (*2–4*). The production of the eyespot pattern is controlled by a developmental organizer called the focus, which induces the surrounding cells to synthesize specific pigments (*5–7*). The evolution of the developmental mechanisms that establish the focus was therefore key to the origin of butterfly eyespots. Here, we identify changes in development and gene expression associated with the evolution of eyespots.

Our screen for genes involved in eyespot evolution was based on the hypothesis that one or more of the signaling molecules that pattern the insect wing blade might also be involved in eyespot development. In *Drosophila*, two orthogonal systems of short-range [Hedgehog (Hh) and Serrate/Delta] and long-range [Decapentaplegic (Dpp) and Wingless (Wg)] signaling proteins organize wing imaginal disc growth, patterning, and gene expression (*8*). If any of these signals were involved in eyespot development, then modulation of their expression patterns near the position of eyespot foci should be observed. To test this hypothesis, we cloned the *Precis coenia* orthologs of the *dpp*, *wg*, and *hh* genes (*9*) and examined their expression patterns by in situ hybridization in fifth (last) larval instar wing imaginal discs, when establishment of the foci occurs (*5*). Only *hh* expression is modulated near developing foci.

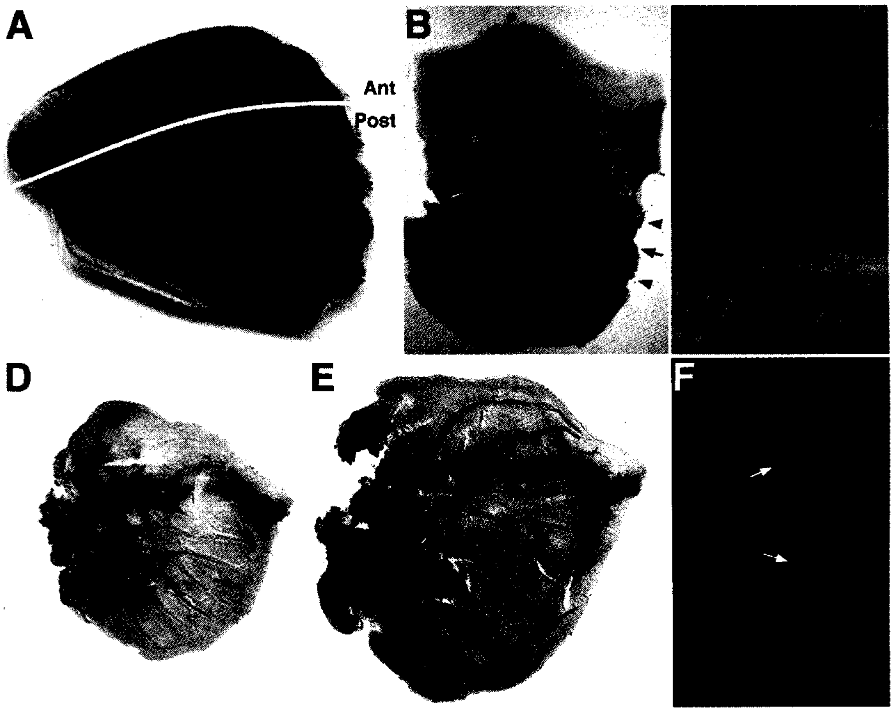

Fig. 1. Hh signal transduction is associated with the establishment of eyespot foci. (**A**) Dorsal surface of the hindwing. The A/P border is indicated (Ant/Post). (**B** and **C**) In situ hybridization with a probe for *hh* RNA. (B) In the mid-fifth instar, *hh* transcripts are detected throughout the posterior compartment. However, *hh* transcription is decreased in the midline (arrow) between the veins (arrowheads) and increased in regions flanking the positions of each potential focus. The heavily stained distal region (damaged in this specimen) is fated for cell death. (C) In the late fifth instar, *hh* transcription is sharply increased in cells flanking those destined to form an active focus (center). No increase is seen in positions that will not form active foci (top and bottom). (**D** and **E**) In situ hybridization with a probe for *ptc* RNA. (D) In the mid-fifth instar, *ptc* transcripts are detected in cells just anterior to the A/P boundary. (E) In the late fifth instar, *ptc* transcripts are also detected in the posterior compartment in eyespot foci (arrows). (**F**) Immunofluorescent detection of Ci protein reveals expression throughout the anterior compartment as well as in the posterior compartment in both eyespot foci (arrows). The anterior part of the wing is toward the top and distal is to the right in all panels.

D. N. Keys, D. L. Lewis, J. E. Selegue, B. J. Pearson, J. Gates, S. B. Carroll, Howard Hughes Medical Institute and Laboratory of Molecular Biology, University of Wisconsin, 1525 Linden Drive, Madison, WI 53706, USA. L. V. Goodrich, R. L. Johnson, M. P. Scott, Howard Hughes Medical Research Institute, Beckman Center, Stanford University Medical Center, Palo Alto, CA 94304, USA.

*These authors contributed equally to this work.

†Present address: Department of Cell Biology, University of Alabama at Birmingham, Birmingham, AL 35294, USA.

‡Present address: Howard Hughes Medical Institute, Eccles Institute of Human Genetics, University of Utah, Salt Lake City, UT 84112, USA.

§To whom correspondence should be addressed. E-mail: sbcarrol@facstaff.wisc.edu